BASIC RF DISCHARGE MODEL

by

M. A. Lieberman

Memorandum No. UCB/ERL M87/65

31 January 1988
(Revised)

BASIC RF DISCHARGE MODEL

by

M. A. Lieberman

Memorandum No. UCB/ERL M87/65

31 January 1988
(Revised)

ELECTRONICS RESEARCH LABORATORY

College of Engineering
University of California, Berkeley
94720

BASIC RF DISCHARGE MODEL

by

M. A. Lieberman

Memorandum No. UCB/ERL M87/65

31 January 1988
(Revised)

ELECTRONICS RESEARCH LABORATORY

College of Engineering
University of California, Berkeley
94720

PREFACE AND ACKNOWLEDGMENT

In medias res. There are certain references to Chapters 2 and 4. These chapters are not yet written. The system of units is the SI (metric) system, except that energies (symbol "$\mathcal{E}$") and temperatures (symbol "T") are given in volts. For energy in joules multiply by $e = 1.6 \times 10^{-19}$ joules/volt. For temperature in kelvins multiply by e/k = 11,600 kelvins/volt.

During the period when this manuscript was written, my studies on plasma-assisted materials processing were supported by National Science Foundation Grant ECS-8517363 and Department of Energy Grant DE-FG03-87ER13727. The assistance provided by these grants is gratefully acknowledged. I thank G. Misium for providing the graphs of atomic collision data used here and for useful comments on the manuscript. I thank A.J. Lichtenberg for carefully reading the manuscript and suggesting many improvements. The original manuscript was the basis for a series of lectures in C.K. Birdsall's graduate course on weakly ionized plasmas at Berkeley. This revision benefited greatly from his comments and those of the graduate students enrolled in his course, in particular Blake Wood and Richard Moroney.

TABLE OF CONTENTS

LIST OF SYMBOLS

A time-varying voltage (or current) is given as V (or I). For sinusoids, $V = \mathrm{Re}\,\tilde{V}\,e^{j\omega t}$, with $\tilde{V}$ (or $\tilde{I}$) being the complex amplitude. The complex amplitude $\tilde{V}$ (or $\tilde{I}$) is written $\tilde{V} = \tilde{V}_0 e^{j\phi_0}$, where $\tilde{V}_0$ (or $\tilde{I}_0$) is the (real) magnitude of $\tilde{V}$ (or $\tilde{I}$), and ϕ_0 is the phase angle in radians.

a (sub), discharge plate

A area

b (sub), discharge plate

B susceptance (siemons)

C capacitance

d plasma length

D diode; (sub) discharge; λ_D, Debye length

e proton charge; (sub) electron

E electric field

$\mathcal{E}$ energy (volts)

f electron speed or energy distribution function; (sub) floating

$\tilde{F}$ complex constant with units of magnetic flux

G conductance (siemons)

i (sub) ion

iz (sub) ionization

I current

$\tilde{I}$ complex current amplitude

$\tilde{I}_0$ real magnitude of complex current amplitude

$\overline{I}$ time-average or dc current

j $\sqrt{-1}$

$\mathbf{J}$ current density

K collision rate constant (m^3–sec^{-1})

l discharge length

L inductance; (sub) loss

m electron mass; (sub) momentum transfer

M ion mass; (sub) matching

n plasma density

N neutral gas density

p pressure; (sub) plasma

P power

$\overline{P}$ time-average power

q collision cross section (m^2)

Q charge

$\mathbf{r}$ position vector

R resistance (ohms)

s sheath thickness; (sub) sheath

t time

T temperature (volts); (sub) Thevenin-equivalent source

u velocity or speed

V voltage

$\tilde{V}$ complex voltage amplitude

$\tilde{V}_0$ real magnitude of complex voltage amplitude

$\bar{V}$ time-average or dc voltage

w sub (wall)

X reactance (ohms)

Y admittance (siemons)

z axial position

Z impedance (ohms)

α first Townsend coefficient

ε dielectric constant

Γ particle flux

λ mean free path (sub e, i); Debye length (sub D)

ν collision frequency

σ electrical conductivity

ϕ phase

Φ electric potential

ω radian frequency

Chapter 3. BASIC RF DISCHARGE MODEL (REVISED)

3.1 Introduction

We describe a uniform, symmetric model for a capacitive parallel plate rf discharge in the regime normally used for reactive ion etching. We call this the "basic model." The principles described in Chapter 2, in particular the conservation laws, are used. Because simplifying assumptions are made, the model cannot be used to predict the quantitative behavior of "real" discharges. The model is correct qualitatively and is introduced to describe the procedure for the analysis of real discharges.

The basic model was developed by V. I. Godyak and his collaborators in the 1970s [Godyak 1972, 1976; Godyak and Kuzovnikov, 1975; Godyak and Popov, 1979]. Certain features of the model were known earlier [Taillet, 1969]. The work of the Soviet group is summarized in a monograph by Godyak (1986). In Chapter 4, we consider nonuniformities and asymmetries in real discharges and examine their effects on the basic model.

Figure 3.1a shows the basic model. A sinusoidal current I_{rf} having complex amplitude $\tilde{I} = \tilde{I}_0 e^{j\phi_0}$ and frequency ω flows across discharge plates a and b. Here $\tilde{I}_0$ is the real magnitude of $\tilde{I}$ and ϕ_0 is the phase of $\tilde{I}$. The plates are separated by a distance l and are taken to be circular, each having cross sectional area A. A gas having neutral density N is present between the plates. In response to the current flow, the gas breaks down and a discharge plasma forms between the plates, accompanied by a voltage $V(t)$ across the plates and a power flow $P(t)$ into the plasma. The plasma has an ion density $n_i(\mathbf{r}, t)$, an electron density $n_e(\mathbf{r}, t)$ and an electron temperature $T_e(\mathbf{r}, t)$. Because of quasineutrality, $n_e \approx n_i$ almost everywhere except within the oscillating sheaths near the plates, where $n_e < n_i$. The instantaneous sheath thickness is $s(t)$ and its time averaged value is $\bar{s}$. Typically, $\bar{s} \ll l$.

The state of the discharge is specified once a complete set of *control parameters* is given. The remaining plasma and circuit parameters are then specified as functions of the control parameters. A convenient choice for the control parameters is $\tilde{I}$, ω, N, and l. Given these, we develop the basic model to determine n_e, T_e, s, $\bar{s}$, V, and P. The choice of control parameters is not unique. We

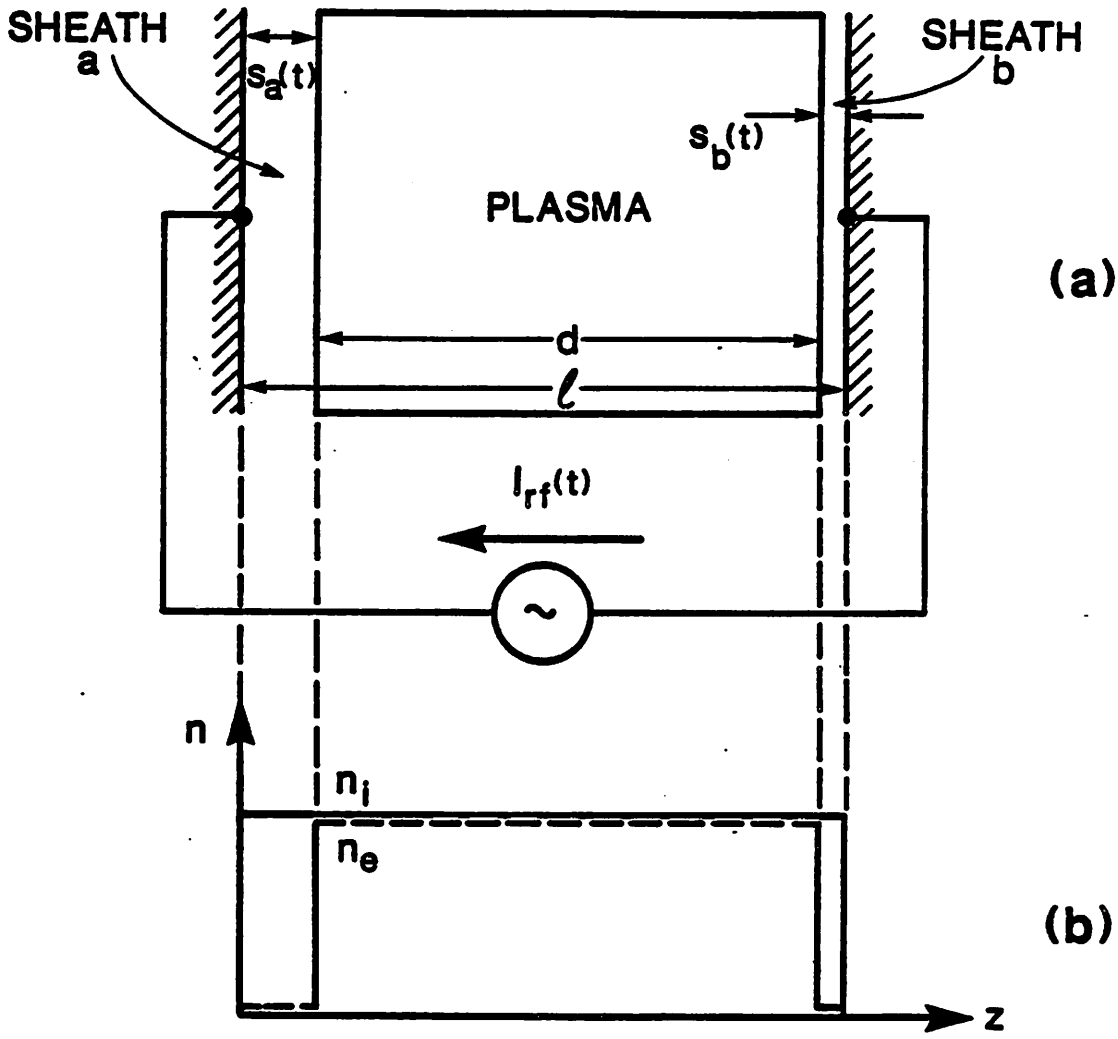

Figure 3.1. The basic rf discharge model. (a) Sheath and plasma thicknesses. (b) Electron and ion densities.

choose I rather than V or P for ease of analysis.

In general, the discharge parameters n_e, n_i, and T_e are complicated functions of position and time. We assume the following to simplify the analysis:

(1) There is no transverse variation (along the plates). This is true provided $l \ll \sqrt{A}$. Since the divergence of Maxwell's equation $\nabla \times \mathbf{H} = \mathbf{J} + \varepsilon_0 \partial \mathbf{E}/\partial t$ is zero, we see that, at any instant of time, the sum of the conduction current $\mathbf{J}$ and the displacement current $\varepsilon_0 \partial \mathbf{E}/\partial t$ within the discharge is independent of z.

(2) The ions respond only to the time-averaged potentials. We will show later that this is true provided that

$$\omega_i^2 \ll \omega^2 , \tag{3.1.1}$$

where ω_i is the ion plasma frequency.

(3) The electrons respond to the instantaneous potentials and carry the rf discharge current. We will show that this is true provided

$$\omega_e^2 \gg \omega^2(1+\nu_m^2/\omega^2)^{1/2} , \tag{3.1.2}$$

where ω_e is the electron plasma frequency and ν_m is the electron-neutral collision frequency for momentum transfer.

(4) The electron density is zero within the sheath regions. This is true provided $\lambda_D \ll s$, where λ_D is the electron Debye length. We will show that this condition is met provided $T_e \ll \overline{V}_{ps}$, where $\overline{V}_{ps}$ is the dc voltage across the sheath.

(5) The ion density is uniform and constant in time everywhere in the plasma and sheath regions. This assumption is made to simplify the analysis and is rarely valid. In the plasma, the density is generally peaked in the center of the discharge and falls to a reduced value at the plasma-sheath boundary. Within the sheath, the density falls further as ions are accelerated toward the discharge plates. These issues are considered in Chapter 4. The electron and ion density profiles for the basic model are shown in Fig. 3.1b.

3.2. Plasma Admittance

The admittance of a plasma slab of thickness d and cross-sectional area A is $Y_p = j\omega\varepsilon_p A/d$, where ε_p is the plasma dielectric constant. From Sec. 2.6,

$$\varepsilon_p = \varepsilon_0\left[1 - \frac{\omega_e^2}{\omega(\omega - j\nu_m)}\right]. \tag{3.2.1}$$

We will show in Sec. 3.3 that

$$d = l - 2\bar{s} = \text{const}, \tag{3.2.2}$$

independent of time. We find that

$$Y_p = j\omega C_0 + \frac{1}{j\omega L_p + R_p}, \tag{3.2.3}$$

where $C_0 = \varepsilon_0 A/d$, $L_p = \omega_e^{-2} C_0^{-1}$ and $R_p = \nu_m L_p$. As shown in Fig. 3.2, Y_p represents a vacuum capacitance C_0 in parallel with the series combination of plasma inductance L_p and resistance R_p. By assumption (3), the displacement current that flows through C_0 is much smaller than the conduction current that flows through L_p and R_p. Thus the element C_0 can be omitted from the model.†

If the sinusoidal current

$$I_{rf}(t) = \text{Re}\,\tilde{I}\, e^{j\omega t} \tag{3.2.4}$$

flows through the plasma, then the voltage across the plasma is given by

$$V_p(t) = \text{Re}\,\tilde{V}_p\, e^{j\omega t}, \tag{3.2.5}$$

where $\tilde{V}_p = \tilde{I}/Y_p$ is the complex voltage amplitude. We see that the plasma voltage is *linear* in the applied current and there is no harmonic generation (multiples of ω) or dc component of V_p.

3.3. Sheath Admittance

In contrast to the plasma, the current that flows through the two sheaths is almost entirely displacement current; i.e., it is due to a time-varying electric field. This is true because the conduction current in a discharge is carried mainly by electrons, and the electron density is zero within the time-

†This holds during normal discharge operation but is not true at startup when $\omega_e \ll \omega$.

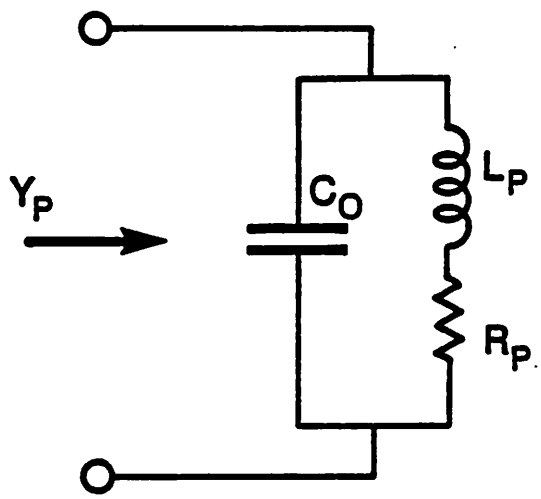

Figure 3.2. **Equivalent circuit model for the plasma.**

varying sheath. We will show that the conduction current carried by the steady flow of ions across the sheath to the plates is much smaller than the displacement current.

3.3.1 *Displacement Current*

The electric field within sheath a (see Fig. 3.1) is given by Poisson's equation

$$\frac{dE}{dz} = \frac{en}{\varepsilon_0} , \quad z \leq s_a(t) , \tag{3.3.1}$$

which yields

$$E(z,t) = \frac{en}{\varepsilon_0} (z - s_a(t)) . \tag{3.3.2}$$

The boundary condition is $E \simeq 0$ at $z = s_a$ because E_{normal} is continuous across the plasma-sheath interface and because a negligible electric field exists in the plasma. E_{normal} is continuous because the discharge cannot support a surface charge (infinite charge density) at the interface.

The displacement current flowing through sheath a into the plasma is

$$I_{ap}(t) = \varepsilon_0 A \frac{\partial E}{\partial t} . \tag{3.3.3}$$

Using (3.3.2) in (3.3.3), we obtain

$$I_{ap}(t) = - enA \frac{ds_a}{dt} . \tag{3.3.4}$$

From (3.3.4), the sheath boundary s_a is *linear* in the applied current. Setting $I_{ap}(t) = I_{rf}(t)$, where

$$I_{rf} = \tilde{I}_0 \cos \omega t , \tag{3.3.5}$$

we integrate (3.3.4) to obtain

$$s_a = \bar{s} - \tilde{s}_0 \sin \omega t \tag{3.3.6}$$

where

$$\tilde{s}_0 = \frac{\tilde{I}_0}{en\omega A} \tag{3.3.7}$$

is the sinusoidal oscillation amplitude about the dc value $\bar{s}$.

The voltage across the sheath is given by

$$V_{ap}(t) = \int_0^{s_a} E\, dz = -\frac{en}{\varepsilon_0}\frac{s_a^2}{2}\,. \tag{3.3.8}$$

From (3.3.8), the sheath voltage is a *nonlinear* function of s_a and therefore of the applied current. Using (3.3.6) in (3.3.8), we obtain

$$V_{ap} = -\frac{en}{2\varepsilon_0}\left[\bar{s}^2 + \frac{1}{2}\bar{s}_0^2 - 2\bar{s}\bar{s}_0 \sin\omega t - \frac{1}{2}\bar{s}_0^2 \cos 2\omega t\right]. \tag{3.3.9}$$

We see that the nonlinearity leads to second harmonic voltage generation.

Differentiating (3.3.8) and using (3.3.4) to eliminate s_a, we obtain

$$I_{ap} = C_a \frac{dV_{ap}}{dt} \tag{3.3.10}$$

where C_a is a *nonlinear* capacitance

$$C_a(V_{ap}) = \frac{A}{(-V_{ap})^{1/2}}\left[\frac{en\varepsilon_0}{2}\right]^{1/2}. \tag{3.3.11}$$

The current flowing through sheath b into the plasma is

$$I_{bp} = -enA\frac{ds_b}{dt}\,, \tag{3.3.12}$$

and the voltage across this sheath is

$$V_{bp} = -\frac{en}{\varepsilon_0}\frac{s_b^2}{2}\,. \tag{3.3.13}$$

By continuity of current, $I_{bp} = -I_{ap}$. Using (3.3.4) and (3.3.12), we obtain

$$\frac{d}{dt}(s_a + s_b) = 0\,,$$

which yields after integration,

$$s_a + s_b = 2\bar{s} = \text{const.} \tag{3.3.14}$$

We see that $d = l - 2\bar{s} = \text{const}$, as stated in Sec. 3.2. For sheath b, we then find

$$s_b = \bar{s} + \tilde{s}_0 \sin \omega t \tag{3.3.15}$$

and a nonlinear voltage response

$$V_{bp} = -\frac{en}{2\varepsilon_0}\left[\bar{s}^2 + \frac{1}{2}\tilde{s}_0^2 + 2\bar{s}\tilde{s}_0 \sin \omega t - \frac{1}{2}\tilde{s}_0^2 \cos 2\omega t\right], \tag{3.3.16}$$

which is modelled by the nonlinear capacitance

$$C_b(V_{bp}) = \frac{A}{(-V_{bp})^{1/2}}\left[\frac{en\varepsilon_0}{2}\right]^{1/2}.$$

Although C_a and C_b are each nonlinear, the voltages across each are related. Substituting (3.3.14) into (3.3.8) and (3.3.13), the combined voltage $V_{ab} = V_{ap} - V_{bp}$ across both sheaths can be written as

$$V_{ab} = \frac{en\bar{s}}{\varepsilon_0}(s_b - s_a). \tag{3.3.17}$$

From (3.3.6) and (3.3.15),

$$V_{ab} = \frac{2en\bar{s}\tilde{s}_0}{\varepsilon_0} \sin \omega t \tag{3.3.18}$$

which is a *linear* voltage response. Differentiating (3.3.17) and using (3.3.4) and (3.3.12) to eliminate s_a and s_b, we obtain the simple result

$$I_{ab} = C_s \frac{dV_{ab}}{dt} \tag{3.3.19}$$

where

$$C_s = \frac{\varepsilon_0 A}{2\bar{s}} \tag{3.3.20}$$

is a *linear* capacitance. Physically, this capacitance is the series combination of the two nonlinear capacitances $C_a = \varepsilon_0 A / s_a(t)$ and $C_b = \varepsilon_0 A / s_b(t)$:

$$\frac{1}{C_a} + \frac{1}{C_b} = \frac{s_a+s_b}{\varepsilon_0 A} = \frac{2\bar{s}}{\varepsilon_0 A} = \frac{1}{C_s} .$$

We obtain the almost paradoxical result that although each sheath is nonlinear, the combined effect of both sheaths is linear. This is true only for the basic model assumptions of a symmetric, homogeneous discharge. We will show in Chapter 4 that the sheath capacitance C_s is nonlinear when these assumptions do not hold.

3.3.2. *Conduction Current*

Although the conduction current in each sheath is small, the average sheath thickness $\bar{s}$ is determined by the balance between ion and electron conduction currents. By assumption (2), there is a steady flow of ions from the plasma through sheath a, carrying a steady current

$$\bar{I}_i = enu_B A \tag{3.3.21}$$

where, from Sec. 2.6, the Bohm velocity

$$u_B = \left[\frac{eT_e}{M}\right]^{1/2} \tag{3.3.22}$$

is the velocity at which ions enter the sheath.

By symmetry, the time average conduction current flowing to plate a is zero. There is a steady flow of ions to the plate. For the basic model, the electron density is strictly zero in the sheath. The sheath thickness $s_a(t)$ must therefore collapse to zero at some time during the rf cycle in order to transfer electrons from the plasma to the plate. It follows from (3.3.6) that

$$\bar{s} = \tilde{s}_0 = \frac{\bar{I}_0}{en\omega A} \tag{3.3.23}$$

and from (3.3.8) that

$$V_{pa} = \frac{en}{2\varepsilon_0}\,\tilde{s}_0^2(1-\sin\omega t)^2 . \tag{3.3.24}$$

Since the sheath voltage collapses to zero at the time that the electrons are transferred to the plate, this action can be modelled as an ideal diode across the sheath whose preferred direction of current flow is

into the plasma. A similar result holds for sheath b.

The voltages $V_{ap}(t)$, $V_{pb}(t)$ and their sum $V_{ab}(t)$ are plotted versus t in Fig. 3.3. The manner in which the sum of the two non-sinusoidal voltages yields the V_{ab} sinusoidal is clearly seen. The time-average value $\overline{V}_{ps}$ for V_{pb} is also shown as the horizontal dashed line.

From the results in Secs. 3.2 and 3.3, we have the circuit model shown in Fig. 3.4. Each sheath is represented as the parallel combination of a nonlinear capacitance C_a or C_b, an ideal diode D, and a dc current source $\overline{I}_i$. The sheath circuits are in series with the plasma circuit shown in Fig. 3.2. Capacitors C_a and C_b are "ganged" together to remind us that their series combination is the linear capacitance C_s.

It will be shown in Sec. 3.5.2 that the ion current source $\overline{I}_i$ represents a flow of dc power out of the discharge. This power is supplied by the rf current source through a rectifying action involving $\overline{I}_i$, D, C_a, and C_b within the sheath. As a result, the rf source "sees" an additional series resistance R_i, which replaces $\overline{I}_i$ and D in the rf circuit model. This model is developed in Sec. 3.6.

Although the circuit form is specified, the elements are functions of the unknown density n and electron temperature T_e. These are determined from conservation of particles and energy as described in the next two sections.

3.4. Ionization Balance

For a steady discharge, the rate of creation of electron-ion pairs is equal to their rate of loss. By quasineutrality, the loss rates for electrons and ions are equal, averaged over an rf cycle. Setting the rate of creation due to electron-neutral ionization equal to the rate of ion loss to the two plates, we obtain

$$n\nu_{iz}Ad = 2nu_BA \ . \tag{3.4.1}$$

The ionization rate ν_{iz} is

$$\nu_{iz} = NK_{iz} \ , \tag{3.4.2}$$

where N is the neutral gas density and

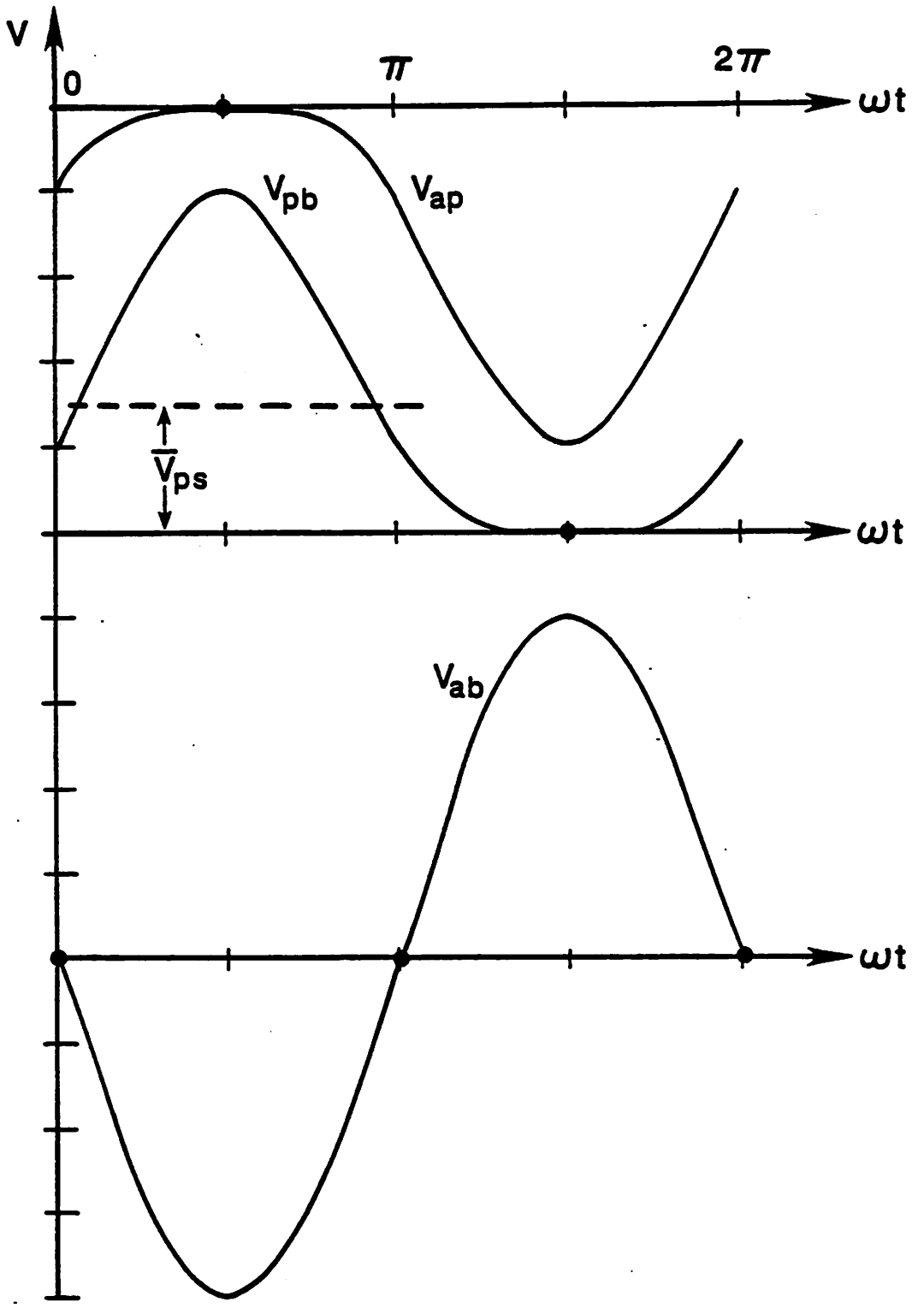

Figure 3.3. Sheath voltages V_{ap}, V_{pb} and their sum V_{ab} versus time. The time-average value $\overline{V}_{ps}$ of V_{pb} is also shown.

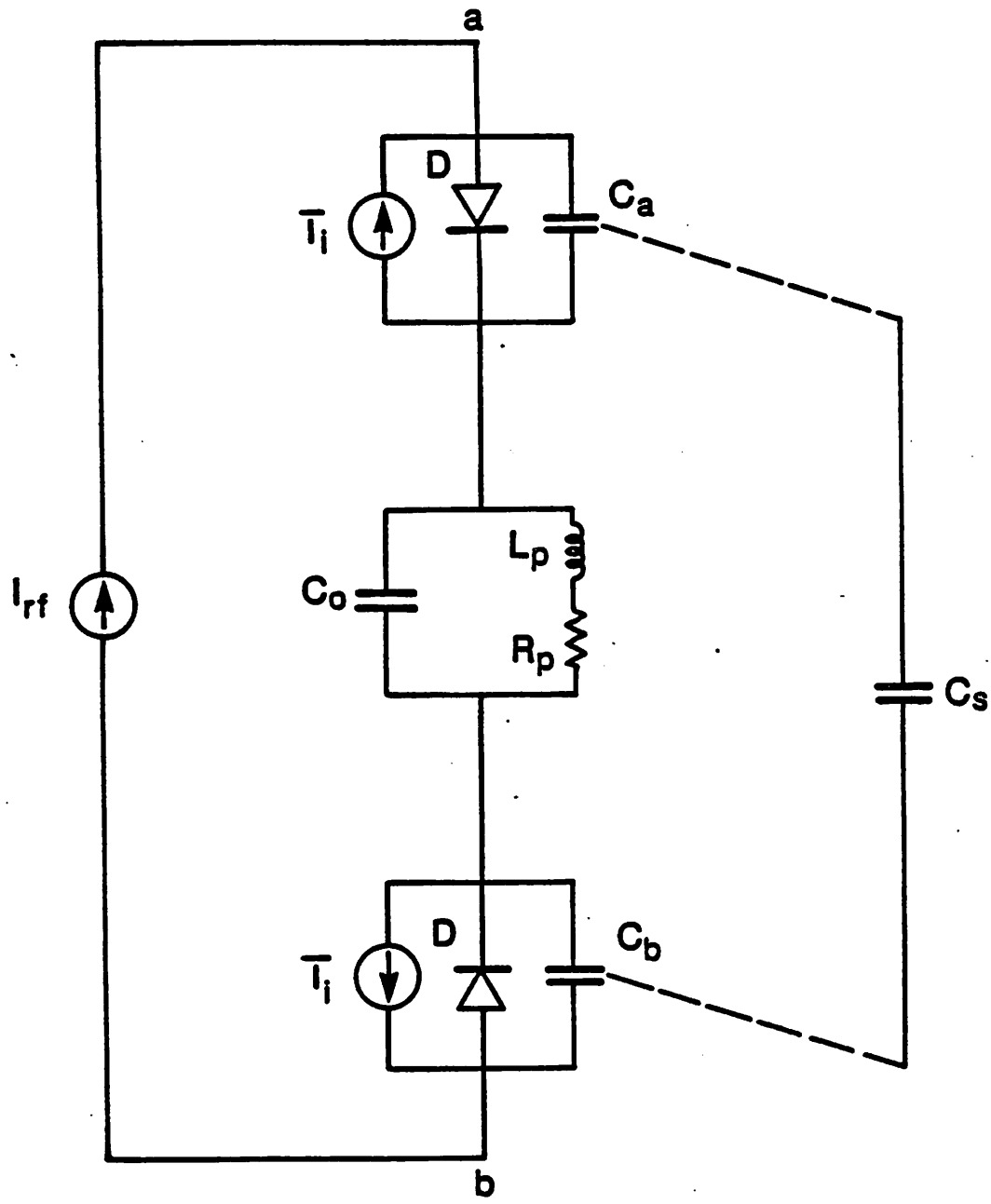

Figure 3.4. Nonlinear circuit model of the rf plasma discharge. The dashed lines indicate that the series connection of the nonlinear elements C_a and C_b yields the corresponding linear element C_s.

$$K_{iz} = \langle q_{iz}(\mathcal{E})u \rangle \tag{3.4.3}$$

is the ionization rate constant. In (3.4.3), q_{iz} is the electron-neutral ionization cross section, u is the electron speed, and the brackets denote an average over the electron energy distribution $f(\mathcal{E})$. For a Maxwellian distribution, K_{iz} is a function of the electron temperature T_e alone. For argon gas, q_{iz} and K_{iz} are plotted in Figs. 3.5 and 3.6 respectively.

Using (3.3.22) and (3.4.2) in (3.4.1), we obtain

$$\boxed{\frac{2}{Nd}\left[\frac{eT_e}{M}\right]^{1/2} = K_{iz}(T_e)\,.} \tag{3.4.4}$$

Since $d = l - 2s$, and generally $s \ll l$, we have $d \approx l$. In this approximation, (3.4.4) determines T_e as a function of the control parameters N and l.

Plotting the left hand side of (3.4.4) on the graph in Fig. 3.6 yields a straight line having slope 1/2 whose vertical position varies with Nd. The intersection of this line with the K_{iz} curve determines T_e. The solid line in Fig. 3.7 shows T_e vs. Nd for argon. Because K_{iz} varies rapidly with T_e, we find that T_e lies between 2 and 5 volts over the many orders of magnitude variation in Nd that are found in typical etching discharges.

We see that there is a *minimum* value $(Nd)_{\min} \approx 1.7 \times 10^{13}$ cm^{-2} to sustain the discharge, shown as the dashed line in Fig. 3.6 which is tangent to the K_{iz} curve. For $d = 5$ cm, we obtain $p_{\min} \approx 10^{-4}$ torr at room temperature in argon.

Because K_{iz} falls off as $T_e^{-1/2}$ for large T_e, we note that there are two solutions to (3.4.4) for $Nd > (Nd)_{\min}$. It can be shown that the solution having the lower value of T_e is stable to perturbations in the discharge parameters, whereas the solution having the higher value of T_e is unstable.

The ionization potential of argon is $\mathcal{E}_{iz} = 15.8$ volts. For T_e between 2 to 5 volts, electron-ion pairs are produced by the small fraction of high energy electrons in the tail of the assumed Maxwellian distribution. The ionization rate is therefore very sensitive to the collisional, heating and loss processes that affect these "tail" electrons. In fact, it is electron-electron scattering that drives the tail electrons toward a Maxwellian distribution, in the face of the other, generally stronger, processes that distort the

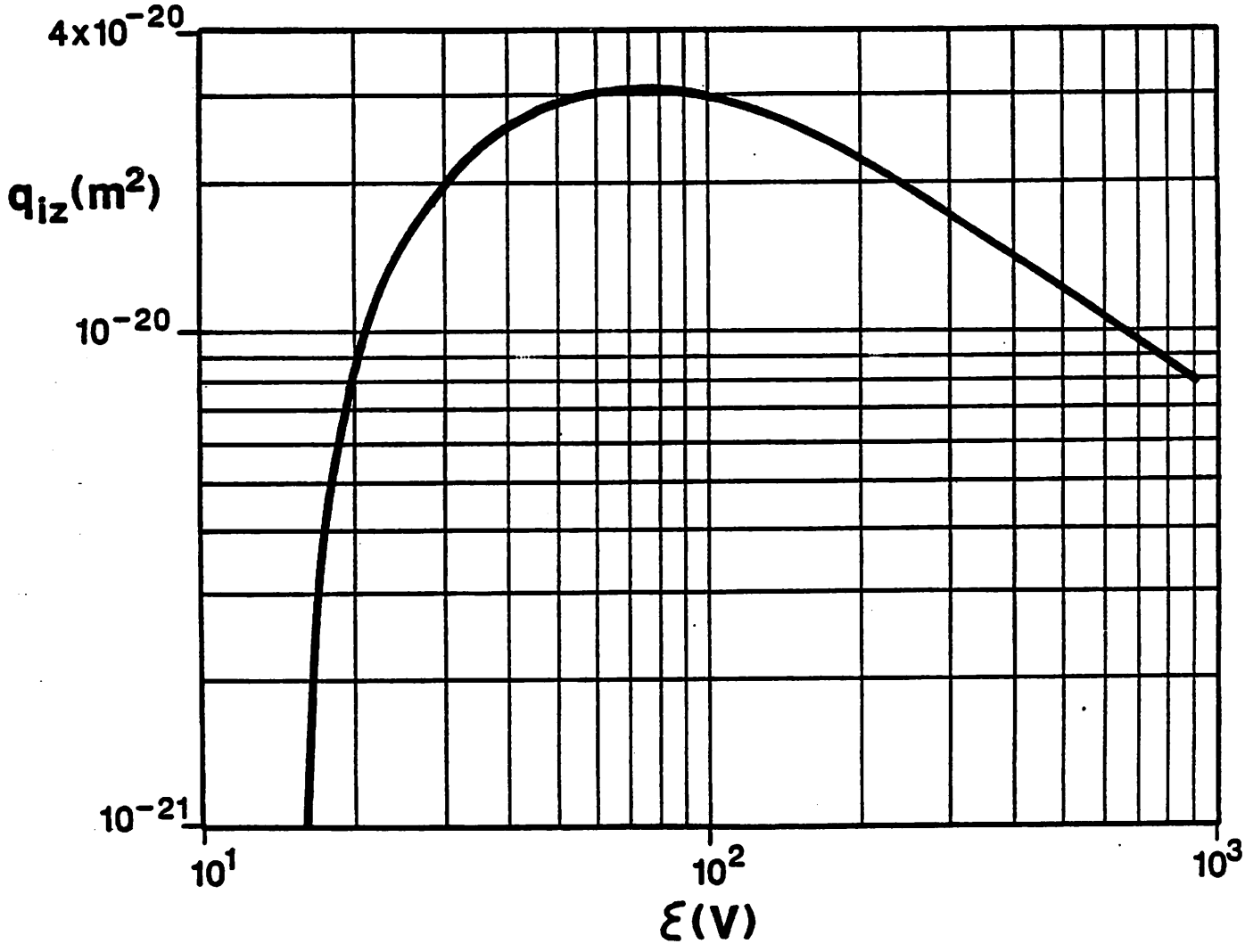

Figure 3.5. Ionization cross section q_{iz} versus electron energy $\mathcal{E}$ for argon gas atoms.

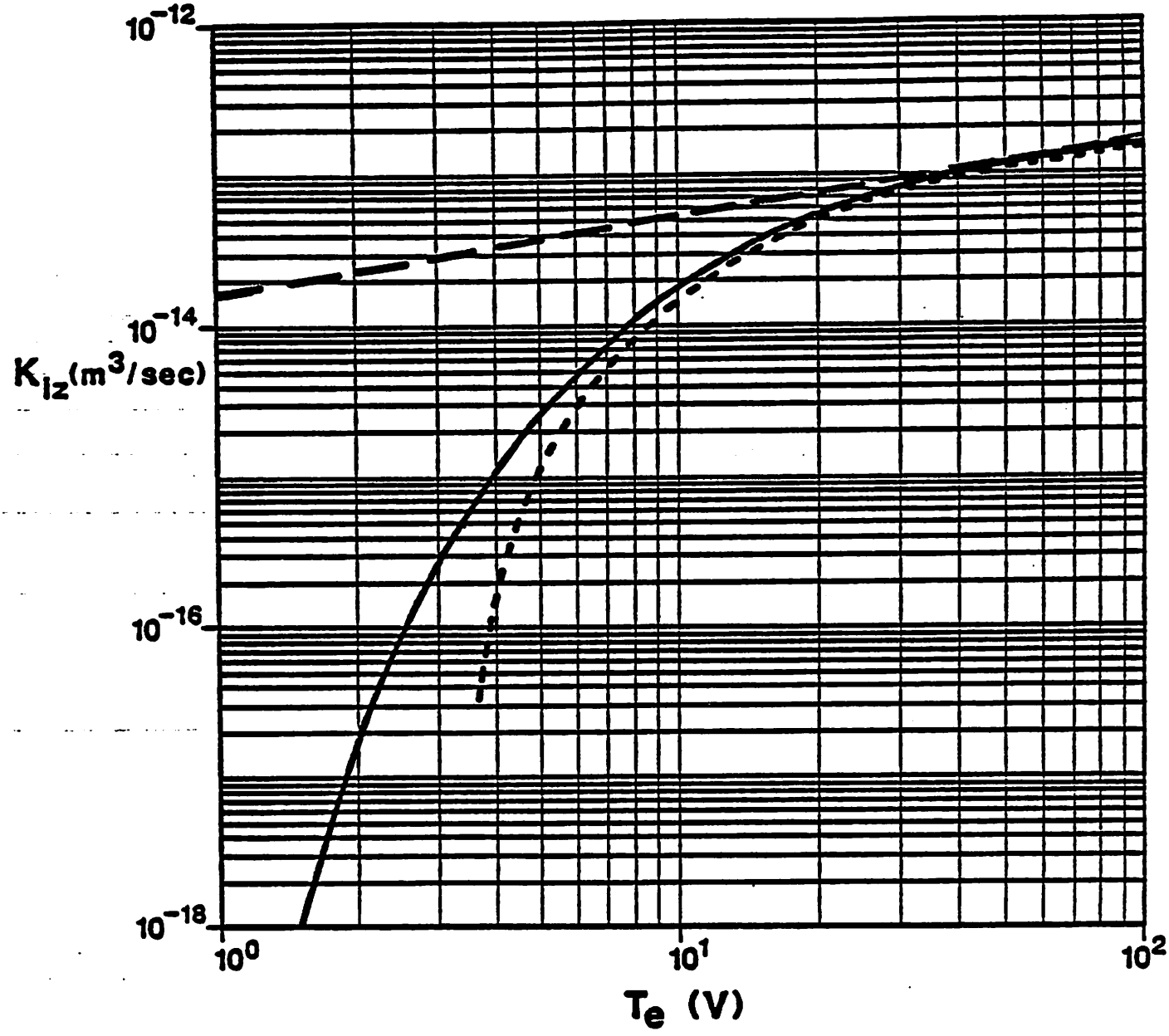

Figure 3.6. Ionization rate constant K_{iz} versus electron temperature T_e for Maxwellian electrons in argon gas. The dashed straight line tangent to the K_{iz} curve defines the minimum value of Nd to sustain the discharge. The dotted curve gives K_{iz} for a Maxwellian electron distribution that is cut off for $\mathcal{E} > 4.7\ T_e$.

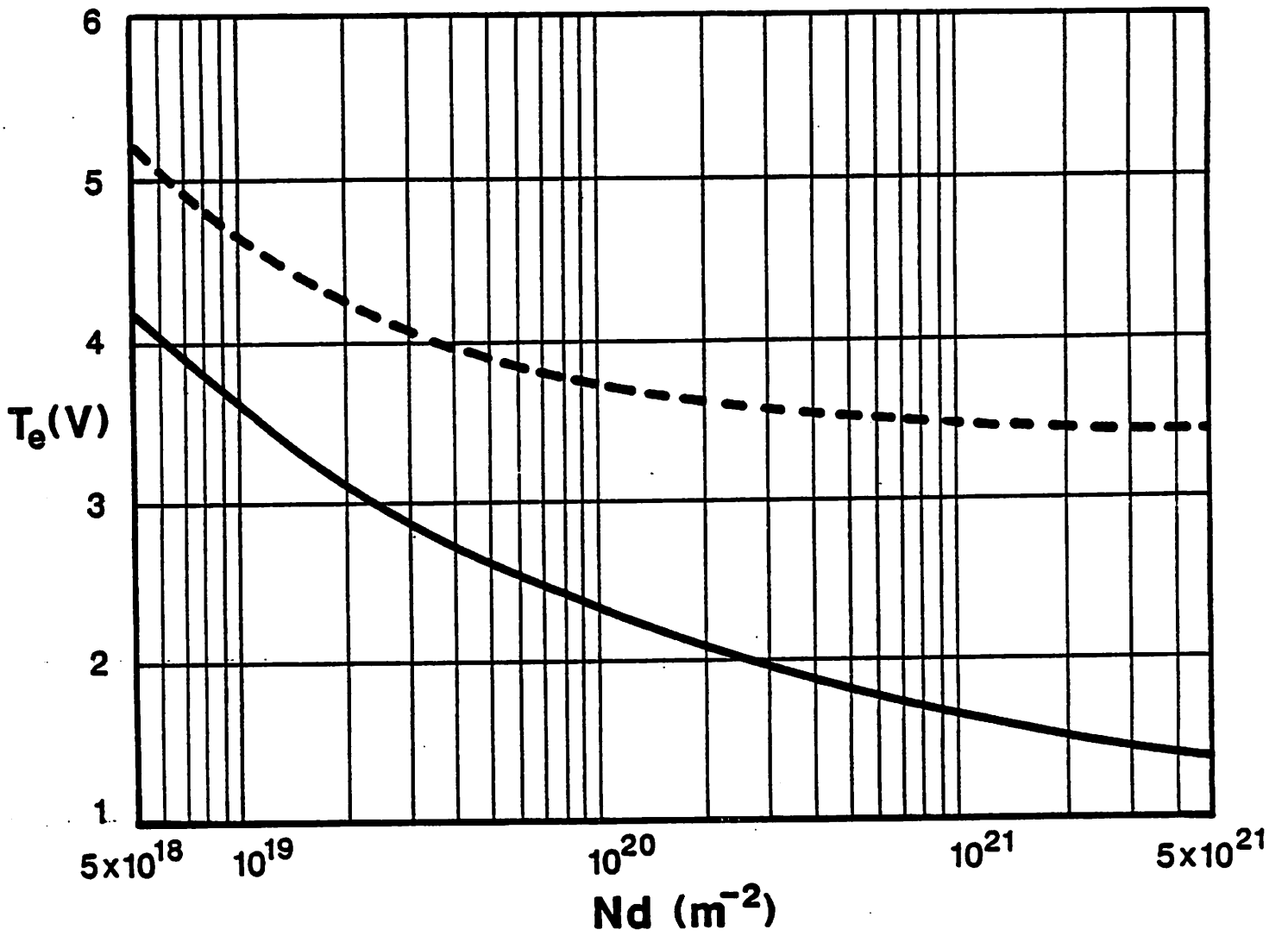

Figure 3.7. Electron temperature T_e versus neutral density-length product Nd in argon gas. The solid curve is for Maxwellian electrons, and the dashed curve is for a Maxwellian distribution truncated at $V_f = 4.7 T_e$ volts.

distribution away from a Maxwellian. If the tail electrons are far from Maxwellian, then the solution to (3.4.4) is only qualitatively correct. A similar difficulty exists in determining the ionization in the positive column of a dc glow discharge. There, ohmic heating competes with energy loss due to elastic and inelastic scattering to determine the equilibrium $f(\mathcal{E})$.

To illustrate the effect of a non-Maxwellian f, we assume that sufficient high energy electrons are lost to the plates to balance the loss of ions to the plates. The equilibrium f is then modelled as a "cutoff" Maxwellian

$$\begin{aligned} f &= f_m(\mathcal{E}) \,, \quad \mathcal{E} < V_f \,; \\ &= 0 \qquad , \quad \mathcal{E} > V_f \,; \end{aligned} \tag{3.4.5}$$

where, from Sec. 2.6,

$$V_f = \frac{1}{2} T_e \ln\left[\frac{M}{2\pi m}\right] \tag{3.4.6}$$

is the floating potential. Integrating q_{iz} for argon ($V_f \approx 4.7\, T_e$) over this f we obtain the ionization rate constant shown as the dotted line in Fig. 3.6. The dotted line in Fig. 3.7 shows the resulting curve of T_e versus Nd. The equilibrium temperatures are higher than for the full Maxwellian, and there is a minimum $T_e \approx 3.4$ V to sustain the discharge.

Although the ionization rate is a rapidly varying function of T_e and is very sensitive to deviations from a Maxwellian distribution, this affects only the particle balance equation (3.4.4). All other equilibrium equations for the basic model depend only weakly on T_e. We can consider T_e to be roughly constant over a wide range of control parameters in these other equations.

3.5. Power Balance

The total time-average power $\overline{P}_{rf}$ absorbed by the discharge is the sum of the power absorbed by the electrons and the power carrried by the ions to the plates.

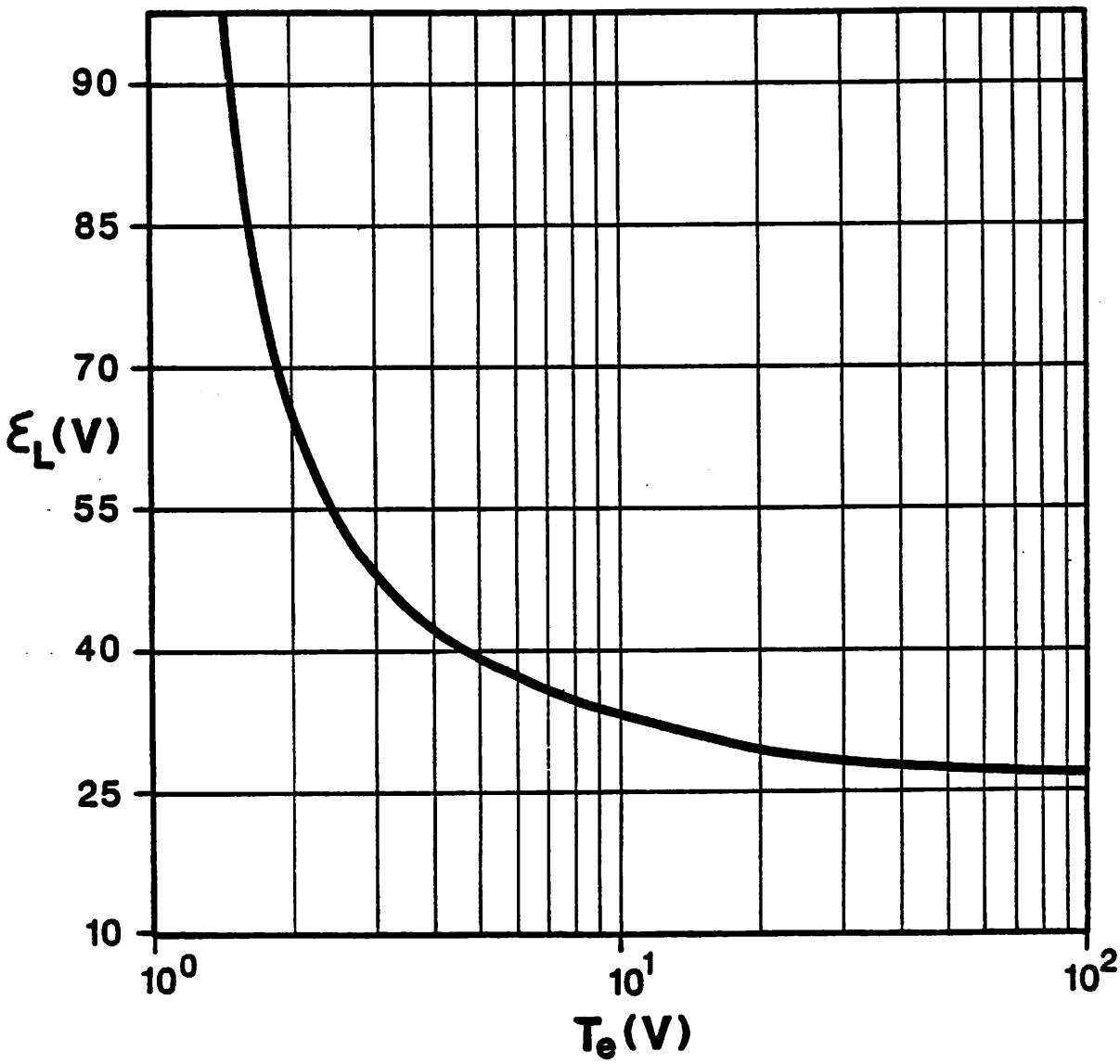

Figure 3.8. Energy loss factor $\mathcal{E}_L$ versus electron temperature T_e in argon gas.

3.5.1. *Electron Power*

The power deposited in the electrons is equal to the power lost by the electrons for a steady discharge. The power deposited is the ohmic heating in the plasma, and the power lost is due mainly to collisional energy transfer to the gas atoms:

$$P_e = \frac{1}{2}\tilde{I}_0^2 R_p = n\nu_{iz} e\,\mathcal{E}_L A d \tag{3.5.1}$$

In (3.5.1), R_p is the plasma resistance (see Fig. 3.4), and it is assumed that essentially all of the source current flows through this element. The quantity $\mathcal{E}_L$ is the electron energy loss per ionization, and accounts for collisional loss due to electron-neutral elastic scattering, electron-neutral excitation and electron-neutral ionization. $\mathcal{E}_L$ is a function of T_e only, and is shown for argon in Fig. 3.8. For T_e in the range typical of etching discharges, $\mathcal{E}_L \approx 3\mathcal{E}_{iz}$. Although electrons are lost to the plates, the power they carry to the plates is relatively small compared to the collisional loss for typical etching discharges.†

From (3.2.3), we find that

$$R_p = \frac{m\nu_m}{e^2 n}\,\frac{d}{A}\,. \tag{3.5.2}$$

We note that

$$\sigma = \frac{e^2 n}{m\nu_m} \tag{3.5.3}$$

is the dc electrical conductivity of the plasma; thus $\frac{1}{2}\tilde{I}_0^2 R_p$ is the time-average ohmic power deposited in the plasma. Inserting $\nu_{iz} = 2u_B/d$ from (3.4.1) into (3.5.1) and using (3.3.7), we obtain

$$\boxed{n = \frac{\tilde{I}_0}{eA\tilde{u}_0}} \tag{3.5.4}$$

†Actually, the kinetic energy per electron lost from the plasma is $2T_e + V_{pb}(t)$, where V_{pb} is the sheath potential at the instant of loss. For $V_{pb} \sim V_f \sim 4.7\,T_e$ and $T_e \sim 5$ V, the energy of lost electrons is not negligible compared to $\mathcal{E}_L$. This additional loss can be included by adding it to $\mathcal{E}_L$ in (3.5.1).

where

$$\tilde{u}_0 = \omega \tilde{s}_0 = \left[\frac{4e\mathcal{E}_L u_B}{m\nu_m d}\right]^{1/2} \tag{3.5.5}$$

is the amplitude of the sheath oscillation velocity.

The momentum transfer frequency ν_m is given by $\nu_m = NK_m$, where K_m is the rate constant for momentum transfer

$$K_m = \langle q_m(\mathcal{E})u \rangle ,$$

q_m is the momentum transfer cross section, and the brackets denote an average over the electron energy distribution. For Maxwellian electrons in argon gas, $q_m(\mathcal{E})$ and $K_m(T_e)$ are shown in Figs. 3.9 and 3.10 respectively. K_m is not sensitive to small deviations from a Maxwellian, and K_m is relatively constant for T_e in the range between 2 and 5 volts.

Assuming that $d \approx l$, (3.5.4) with (3.5.5) gives the plasma density n as a function of the control parameters $\tilde{I}$, N and l. In addition, n depends weakly on T_e, already determined as a function of the control parameters in Sec. 3.4.

Inserting (3.4.1) into (3.5.1), the electron power is

$$P_e = 2nu_B Ae\mathcal{E}_L \tag{3.5.6}$$

Using (3.5.4) and (3.5.5) in (3.5.6),

$$P_e = 2\frac{u_B}{\tilde{u}_0}\tilde{I}_0\mathcal{E}_L . \tag{3.5.7}$$

Equating (3.5.7) to the left hand side of (3.5.1), we obtain

$$R_p = 4\frac{u_B}{\tilde{u}_0}\frac{\mathcal{E}_L}{\tilde{I}_0} . \tag{3.5.8}$$

The resistance R_p due to electron power loss decreases as $\tilde{I}_0$ increases because, from (3.5.4), the carrier density increases with $\tilde{I}_0$.

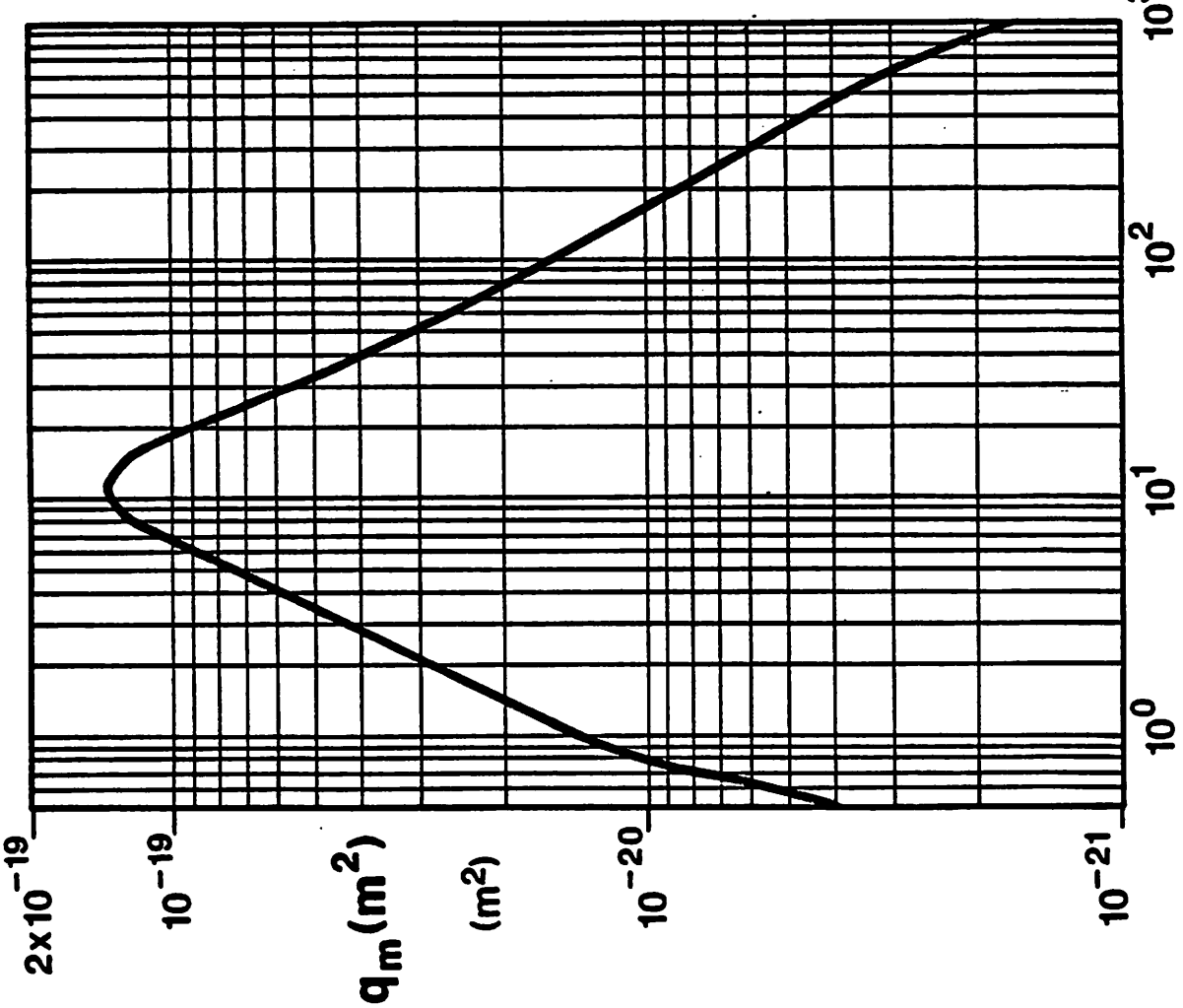

Figure 3.9. Momentum transfer cross section q_m versus electron energy $\mathcal{E}$ for argon gas atoms.

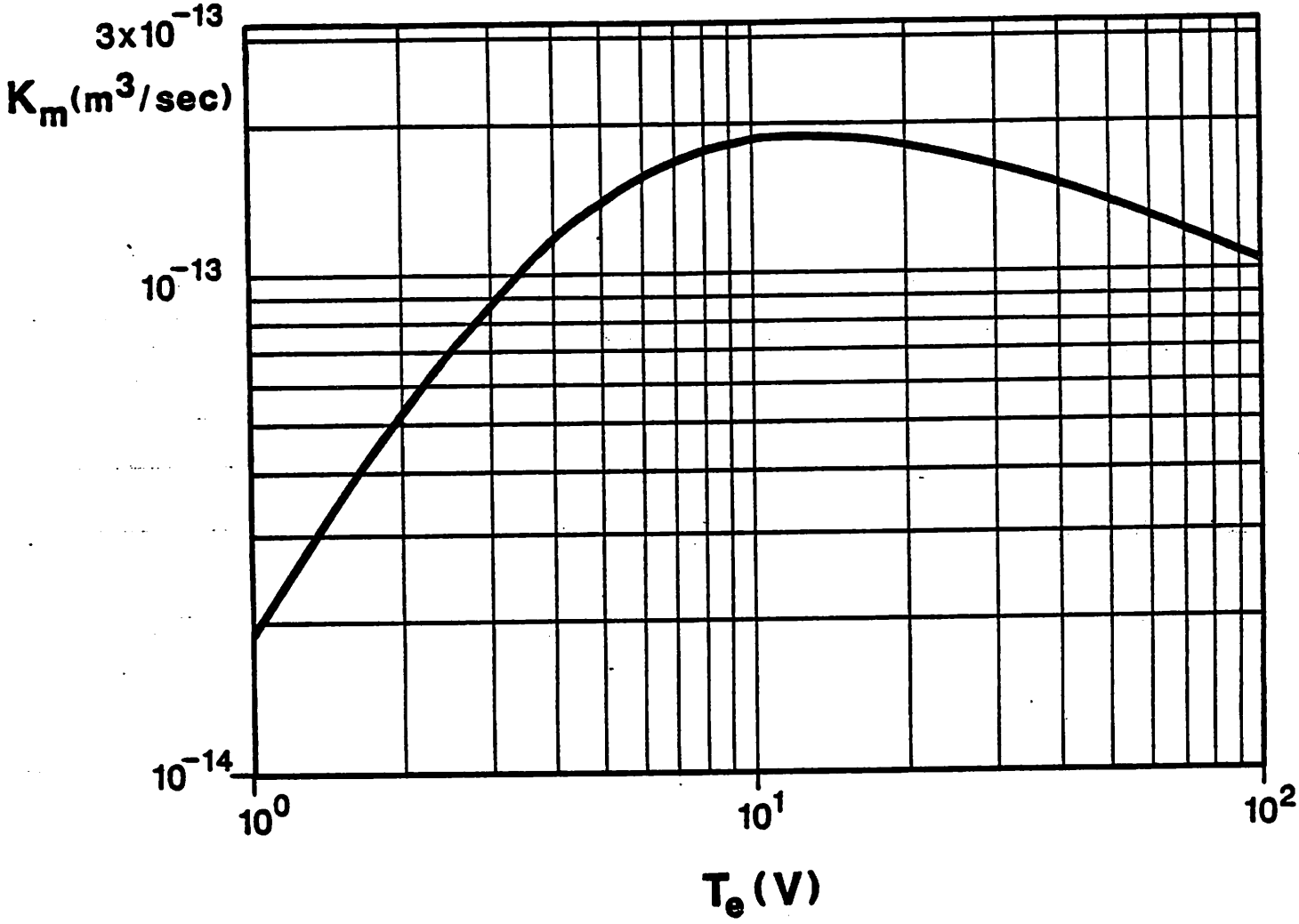

Figure 3.10. Momentum transfer rate constant K_m versus electron temperature T_e for Maxwellian electrons in argon gas.

3.5.2 *Ion Power*

The power carried by the ions to the plates is

$$P_i = 2nu_B Ae\bar{V}_{ps} \tag{3.5.9}$$

where $2\bar{I}_i = 2nu_B Ae$ is the total dc ion current and $\bar{V}_{ps}$ is the dc sheath voltage. Averaging (3.3.9) over time and using (3.3.7), we obtain

$$\boxed{\bar{V}_{ps} = \frac{3en}{4\varepsilon_0}\left[\frac{\tilde{I}_0}{en\omega A}\right]^2} . \tag{3.5.10}$$

Substituting (3.5.10) in (3.5.9), we obtain

$$P_i = \frac{3\tilde{I}_0^2 u_B}{2\varepsilon_0\omega^2 A} . \tag{3.5.11}$$

Writing $P_i = \frac{1}{2}\tilde{I}_0^2 R_i$, we obtain from (3.5.11) the effective resistance due to ion power losses

$$R_i = \frac{3u_B}{\varepsilon_0\omega^2 A} . \tag{3.5.12}$$

Summing (3.5.7) and (3.5.11), we obtain the total time-average power supplied to the discharge

$$\bar{P}_{rf} = 2\frac{u_B}{\bar{u}_0}\tilde{I}_0\mathcal{E}_L + \frac{3\tilde{I}_0^2 u_B}{2\varepsilon_0\omega^2 A} . \tag{3.5.13}$$

The dc ion power is supplied by the rf source by means of a rectifying action, as follows: Electron-ion pairs are continuously created by ionization. During most of the rf cycle, ions flow steadily to each plate without an accompanying flow of electrons. The ions accumulate on the plate. Since the plasma is quasineutral, the excess electrons created by ionization are transported to the plasma-sheath boundaries, where they accumulate. The electron accumulation causes both sheaths to diminish in thickness at the velocity u_B; if unchecked, the sheaths would collapse. However, the rf source alternately drives boundary a into plate a and boundary b into plate b. When boundary a strikes plate a, the excess electrons suddenly flow to the plate to neutralize the ions. These electrons are supplied by the plasma, causing the sheath at boundary b to suddenly expand. A half-period later,

the sheath at boundary b strikes plate b, and, in turn, sheath a suddenly expands. This cycle repeats continually.

To determine quantitatively the time-average rf power supplied by the source during this cycle, we let $I_{rf} = -\tilde{I}_0 \sin \omega t$, and we introduce the periodic sawtooth function

$$\text{saw}(\phi) = 1 - \frac{\phi}{\pi}, \quad 0 \le \phi < 2\pi, \tag{3.5.14}$$

where saw(ϕ) is an odd function periodic in ϕ with period 2π. From the preceding description of sheath motion we can write

$$s_a(t) = \bar{s}_0(1-\cos \omega t) + \frac{\pi u_B}{\omega} \text{saw}(\omega t - \pi), \tag{3.5.15}$$

$$s_b(t) = \bar{s}_0(1+\cos \omega t) + \frac{\pi u_B}{\omega} \text{saw}(\omega t), \tag{3.5.16}$$

such that

$$s_a + s_b = 2\bar{s}_0 + \frac{\pi u_B}{\omega} \text{saw}(2\omega t). \tag{3.5.17}$$

The charge Q_a on plate a is due to both the source current I_{rf} and the electron and ion conduction currents:

$$Q_a(t) = \frac{\tilde{I}_0}{\omega} \cos \omega t + \frac{\pi \bar{I}_i}{\omega} (1-\text{saw}(\omega t)). \tag{3.5.18}$$

The voltage across both sheaths is

$$V_{rf}(t) = Q_a(t)/C(t), \tag{3.5.19}$$

where $C(t) = \varepsilon_0 A/(s_a+s_b)$ is the time-varying sheath capacitance. The instantaneous power is then $P(t) = V_{rf} I_{rf}$. Taking the time average of P using (3.5.14) and (3.5.17)-(3.5.18), we obtain

$$\bar{P}_{rf} = \frac{3\tilde{I}_0^2 u_B}{2\varepsilon_0 \omega^2 A}, \tag{3.5.20}$$

which is identical to P_i given in (3.5.11). For I_{rf} a sinusoid, we note that V_{rf} contains higher har-

monics of ω, but this anharmonic content of V_{rf} is of order $\bar{I}_i/\tilde{I}_0 \ll 1$.

3.6. Circuit Laws

The voltage amplitude $\tilde{V}$ is determined from the rf circuit equations. The circuit is the series combination of the ion resistance R_i, the electron resistance R_p, the plasma inductance L_p, and the total sheath capacitance C_s. R_i is a constant resistance, independent of $\tilde{I}_0$. However, R_p and L_p are both inversely proportional to n [see (3.2.3)]. Since $n \propto \tilde{I}_0$ from (3.5.4), the complex amplitude $\tilde{V}_p$ of the voltage across these elements is

$$\tilde{V}_p = (j\omega L_p + R_p)\,\tilde{I}\ , \tag{3.6.1}$$

or

$$\tilde{V}_p = (j\omega + \nu_m)\,\tilde{F}\ , \tag{3.6.2}$$

where

$$\tilde{F} = \frac{m\tilde{u}_0 d}{e}\, e^{j\phi_0} \tag{3.6.3}$$

is a complex constant. We recall that $\tilde{I} = \tilde{I}_0 e^{j\phi_0}$, with ϕ_0 some arbitrary reference phase. Thus $\tilde{V}_p$ is a constant, independent of $\tilde{I}_0$. This represents a sinusoidal voltage source

$$V_p(t) = \mathrm{Re}\,\tilde{V}_p e^{j\omega t} \tag{3.6.4}$$

which has a component proportional to ν_m that is in phase with the current. This in-phase component absorbs the electron power P_e.

Finally, the capacitance C_s is, using (3.3.20), (3.3.23), and (3.5.4)

$$C_s = \frac{\varepsilon_0 A\,\omega}{2\tilde{u}_0}\ . \tag{3.6.5}$$

The equivalent circuit for these elements is shown in Fig. 3.11, and has the V–I relation

$$\tilde{V} = \tilde{I}R_i + \frac{\tilde{I}}{j\omega C_s} + j\omega\tilde{F} + \nu_m\tilde{F}\ . \tag{3.6.6}$$

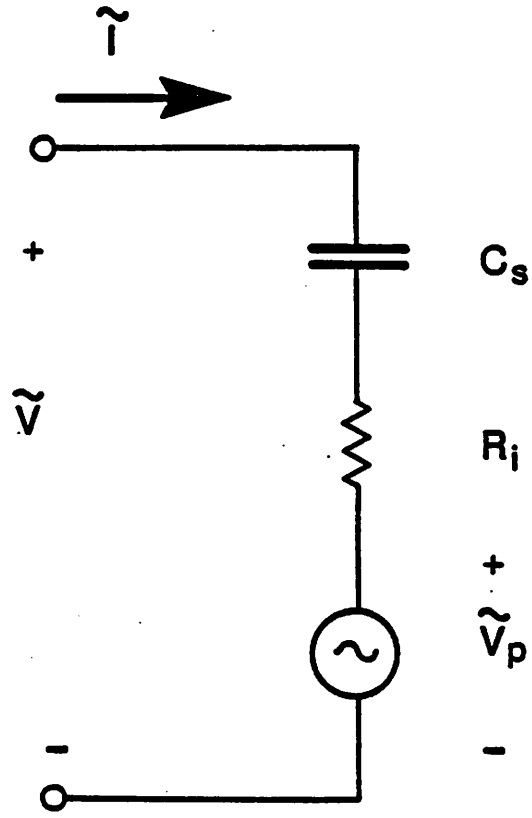

Figure 3.11. **Rf equivalent circuit for the capacitive discharge.**

where $\tilde{V}$ is the total discharge voltage amplitude and $\tilde{I}$ is the discharge current amplitude.

At the driving frequencies for typical etching discharges (13.56 MHz and below), the second term in (3.6.6) is large compared to the other terms, and the discharge is *capacitive*. As the frequency is increased, the condition of series *resonance* is reached, where the sum of the second and third terms is zero:

$$\omega_{res} = \left[\frac{2e\tilde{I}_0}{m\varepsilon_0 A d}\right]^{1/3} .$$

The voltage across the discharge has the minimum value

$$\tilde{V}_{\min} = \tilde{I}R_i + \nu_m \tilde{F} \tag{3.6.7}$$

Above the resonant frequency, the discharge is *inductive*. For a capacitive discharge, $\omega \ll \omega_{res}$, (3.6.6) reduces to

$$\boxed{\tilde{V} = \frac{2\tilde{u}_0 \tilde{I}}{j\omega^2 \varepsilon_0 A} .} \tag{3.6.8}$$

The dc voltage across sheath a or b is obtained by time-averaging (3.3.9) for $\overline{s} = \overline{s}_0$:

$$\overline{V}_{ps} = \frac{3en}{4\varepsilon_0} \overline{s}_0^2 . \tag{3.6.9}$$

The rf voltage amplitude across a capacitive discharge is obtained from (3.3.18):

$$|\tilde{V}| = \tilde{V}_{ab} = \frac{2en}{\varepsilon_0} \overline{s}_0^2 . \tag{3.6.10}$$

From (3.6.9) and (3.6.10),

$$\boxed{\overline{V}_{ps} = \frac{3}{8} |\tilde{V}| .} \tag{3.6.11}$$

This is shown as the dashed line in Fig. 3.3.

Finally, writing $d = l - 2\overline{s}$ and using (3.3.23) and (3.5.4), we obtain

$$\boxed{d = l - \frac{2\tilde{u}_0}{\omega}} \quad . \tag{3.6.12}$$

The boxed equations (3.4.4), (3.5.4), (3.5.13), (3.6.8), (3.6.11), and (3.6.12), along with (3.5.5) for $\tilde{u}_0 = \omega\tilde{s}_0$, comprise the *basic model* for the capacitive rf discharge. The equations determine T_e, n, $\bar{P}_{rf}$, $\tilde{V}$, $\bar{V}_{ps}$, $\tilde{u}_0$, $\tilde{s}_0 = \bar{s}$, and d as functions of the control parameters $\tilde{I}$, ω, N and l. For comparison with experimental results, it is usually more convenient to choose $\bar{P}_{rf}$ as the electrical control parameter rather than I_{rf}. The procedure for solving the basic model is then as follows:

1. Approximating $d \simeq l$, we solve (3.4.4) for T_e.
2. Using T_e in (3.5.5), we obtain $\tilde{u}_0$.
3. For the given $\bar{P}_{rf}$, we solve (3.5.13) for $\tilde{I}_0$.
4. Using $\tilde{u}_0$ and $\tilde{I}_0$ in (3.5.4) and (3.6.8), we obtain n and $\tilde{V}$.
5. Equation (3.6.11) then yields $\bar{V}_{ps}$.
6. Finally, we determine d using (3.6.12) and verify that $d \simeq l$.
7. If this is not the case, then we iterate the procedure using the new value of d. This iteration converges very rapidly.

Although there is no difficulty solving the quadratic equation (3.5.13) for $\tilde{I}_0$, it is instructive to consider the two limiting cases of mainly ion or mainly electron power loss. The two terms on the right hand side of (3.5.13) are equal for

$$P_{rf0} = \frac{4}{3}\frac{m}{e}\varepsilon_0 K_m \mathcal{E}_L \; \omega^2 N d \; A \quad . \tag{3.6.13}$$

Fixing T_e and approximating $d = l$, we obtain the following scalings with ω, $\bar{P}_{rf}$, A, and Nl:

(1) Ion power loss, $\bar{P}_{rf} \gg \bar{P}_{rf0}$. Comparing (3.5.6) and (3.5.9), we see that the voltage is high; $\bar{V}_{ps} \gg \mathcal{E}_L$. Using $\nu_m \propto N$ and $\tilde{u}_0 \propto (Nl)^{-1/2}$, we obtain

$$\tilde{I}_0 \propto \omega \, \bar{P}_{rf}^{1/2} \, A^{1/2} \, , \tag{3.6.14}$$

$$n \propto \omega \, \bar{P}_{rf}^{1/2} \, A^{-1/2} \, (Nl)^{1/2} \, , \tag{3.6.15}$$

$$\tilde{V} \propto \omega^{-1} \bar{P}_{rf}^{1/2} A^{-1/2} (Nl)^{-1/2} . \tag{3.6.16}$$

(2) Electron power loss, $\bar{P}_{rf} \ll \bar{P}_{rf0}$. The voltage is low, $\bar{V}_{ps} \ll \mathcal{E}_L$. We obtain

$$\tilde{I}_0 \propto \bar{P}_{rf} (Nl)^{-1/2} , \tag{3.6.17}$$

$$n \propto \bar{P}_{rf} A^{-1} , \tag{3.6.18}$$

$$\tilde{V} \propto \omega^{-2} \bar{P}_{rf} A^{-1} (Nl)^{-1} . \tag{3.6.19}$$

3.7. Matching Networks

If the discharge is driven directly by an rf power source, then generally power is not transferred efficiently from the source to the discharge. As shown in Fig. 3.12, the discharge is modeled as a load having impedance $Z_D = R_D + jX_D$, where $R_D = R_i + \tilde{V}_p/\tilde{I}$ is the discharge resistance and $X_D = -(\omega C_s)^{-1}$ is the discharge reactance. The power source is modeled by its Thevenin-equivalent circuit, consisting of a voltage source $\tilde{V}_T$ in series with a source resistance R_T. The power flowing into the discharge is

$$\bar{P}_{rf} = \frac{1}{2} \mathrm{Re}(\tilde{V} \tilde{I}^*) . \tag{3.7.1}$$

Solving the circuit in Fig. 3.12 for $\tilde{I}$ and $\tilde{V}$, we obtain

$$\tilde{I} = \frac{\tilde{V}_T}{R_T+R_D+jX_D} , \tag{3.7.2}$$

$$\tilde{V} = \tilde{I}(R_D+jX_D) . \tag{3.7.3}$$

Using (3.7.2) and (3.7.3) in (3.7.1), we obtain

$$\bar{P}_{rf} = \frac{1}{2} |\tilde{V}_T|^2 \frac{R_D}{(R_T+R_D)^2+X_D^2} \tag{3.7.4}$$

Fixing the source parameters $\tilde{V}_T$ and R_T, what values of the load parameters R_D and X_D will maximize $\bar{P}$? Setting $\partial\bar{P}/\partial X_D = 0$ and $\partial\bar{P}/\partial R_D = 0$, we obtain $X_D = 0$ and $R_D = R_T$ for maximum power transfer. The load $Z_D = R_T$ is call a *matched load.* The maximum power supplied by the

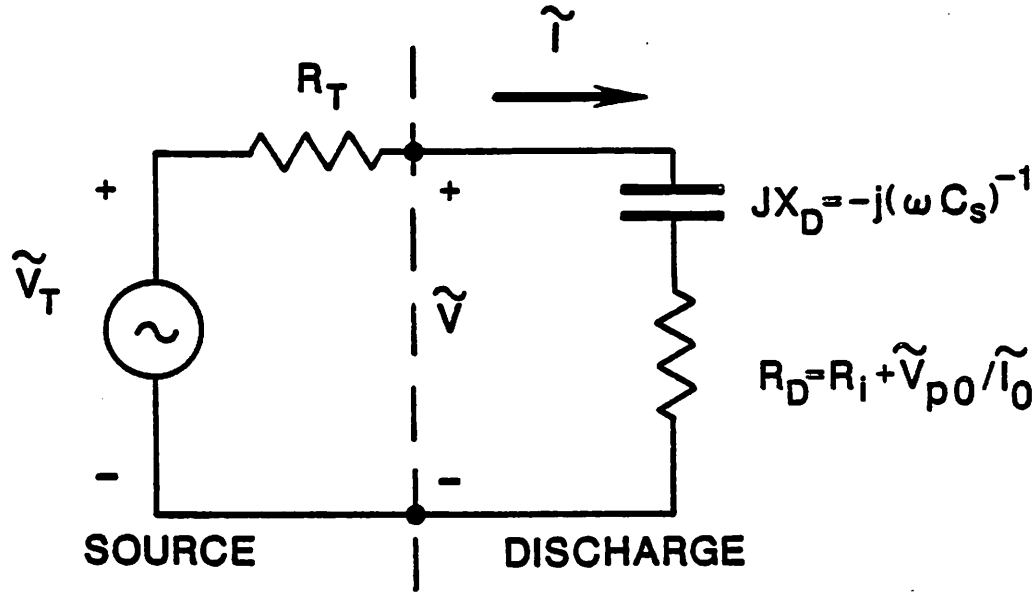

Figure 3.12. Equivalent circuit to determine time-average rf power.

source to the load is then

$$\bar{P}_{\max} = \frac{1}{4} \frac{|\tilde{V}_T|^2}{R_T} . \tag{3.7.5}$$

Since the discharge impedance Z_D is usually much smaller than R_T, the power $\bar{P}_{rf}$ is generally much less than $\bar{P}_{\max}$. To increase $\bar{P}_{rf}$ to $\bar{P}_{\max}$, a lossless matching network is usually placed between the source and the discharge. Because R_D and X_D are two independent components of Z_D, the simplest matching network consists of two independent components. The most common configuration, called the "L-network," is shown in Fig. 3.13. It consists of a shunt capacitor having susceptance $B_M = \omega C_M$ and a series inductor having a reactance $X_M = \omega L_M$.

To understand the operation of the matching network, we refer to the complex impedance plane shown in Fig. 3.14. In this plane, the locus of an impedance having constant resistance is a vertical straight line having ordinate R, and the locus of an impedance having a constant conductance G is a circle of radius $(2G)^{-1}$ whose center is at $X = 0, R = (2G)^{-1}$.† This circle always touches the origin. A typical discharge impedance is plotted as point 1 in the figure. Usually $R_D < R_T$ and X_D is negative for a capacitance discharge.

To match the source to the load, we adjust X_M so that the impedance Z_2 (see Fig. 3.13) has a conductance $G_2 = 1/R_T$. Because $Z_2 = R_D + j(X_M+X_D)$, this corresponds to moving from 1 to 2 along the constant resistance locus in Fig. 3.14 having ordinate R_D. We next adjust B_M so that the admittance Y_3 (see Fig. 3.13) has $B_3 = 0$. Because $Y_3 = 1/R_T + j(B_2+B_M)$, this corresponds to moving from 2 to 3 along the constant conductance circle $G = G_T$. This achieves the matched condition, i.e., the Thevenin-equivalent source "sees" an impedance R_T.

To determine X_M and B_M, we write

---

†To see the latter, we write $R + jX = (G+jB)^{-1}$, which yields $R = G/(G^2+B^2)$ and $X = -B/(G^2+B^2)$. Fixing G, we note that

$$[R(B) - (2G)^{-1}]^2 + X^2(B) = (2G)^{-2}$$

for any B, which is the equation of the circle as stated.

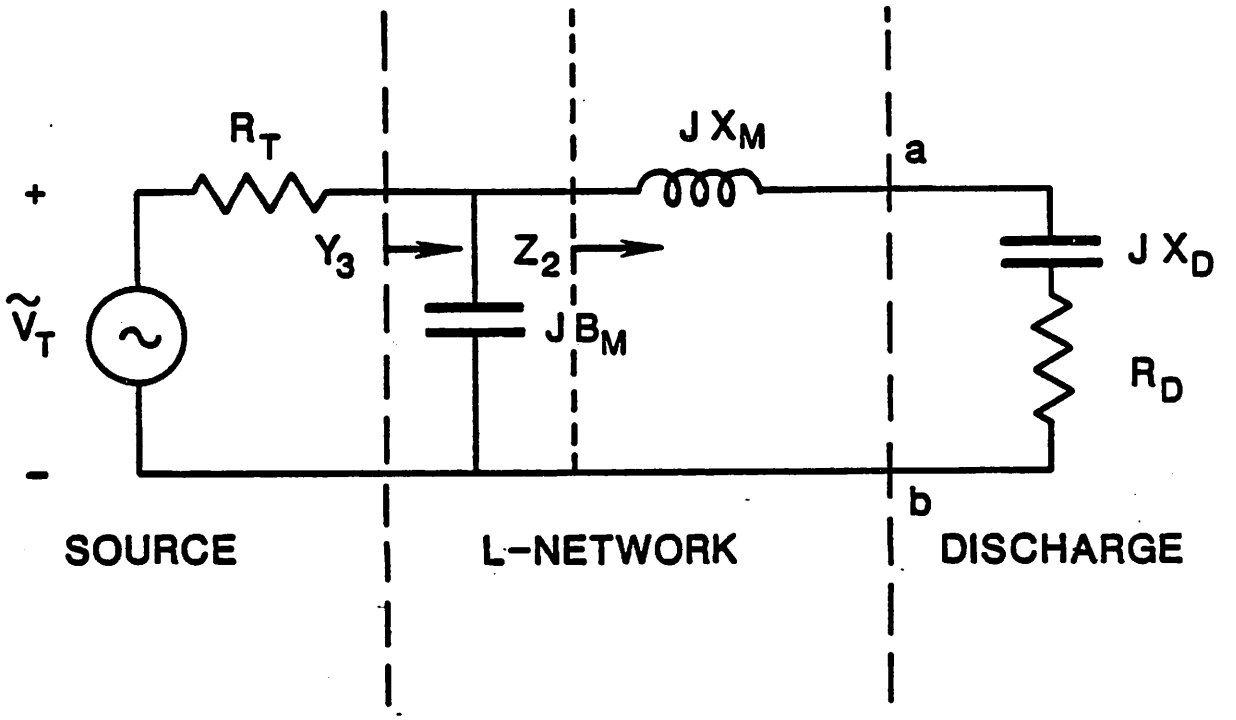

Figure 3.13. Equivalent circuit for matching the rf power source to the discharge using an L-network.

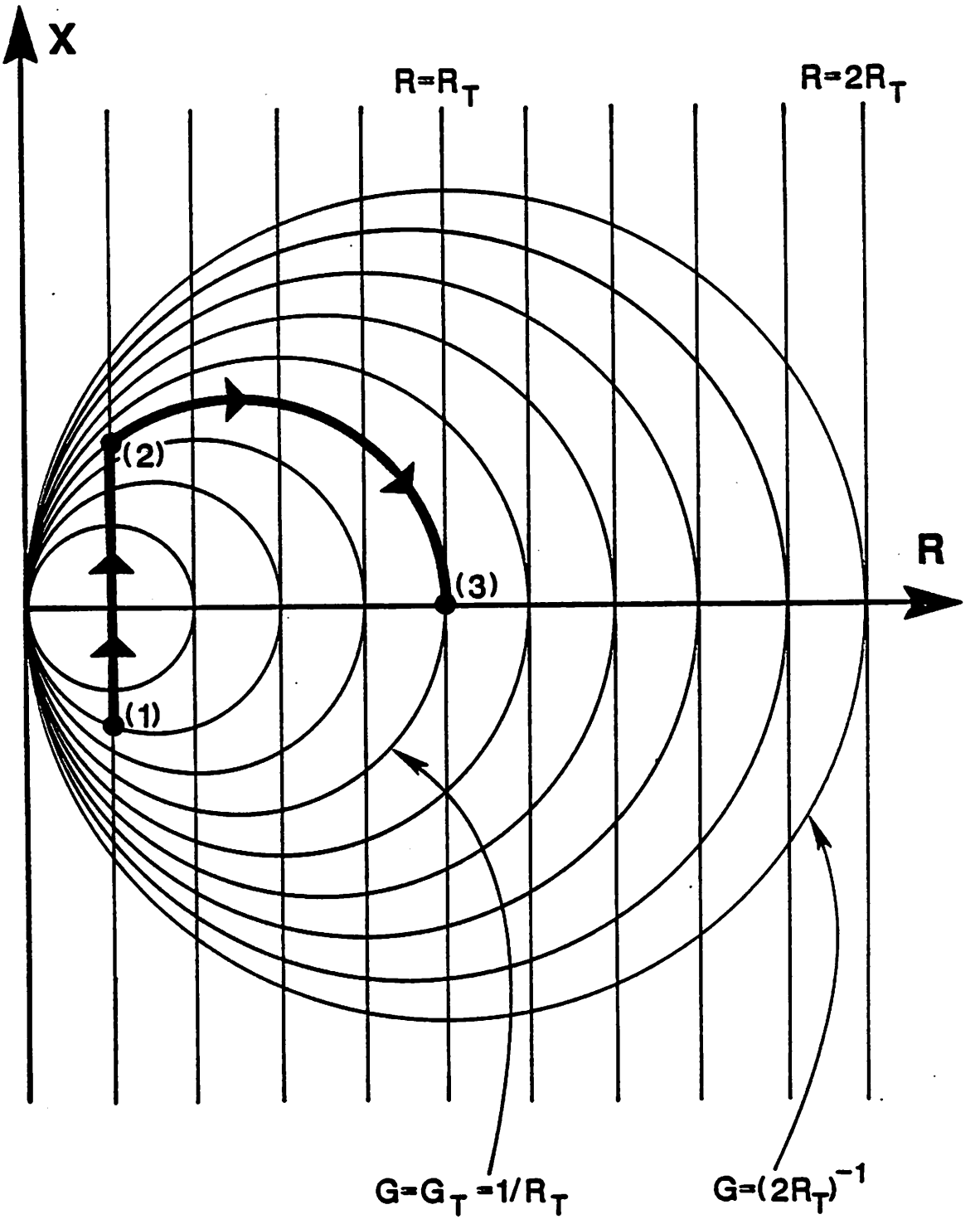

Figure 3.14. Complex impedance plane X versus R. The loci of constant resistance R and conductance G are shown. The heavy solid line from (1) to (3) shows the locus for matching the source to the discharge using the L-network.

$$G_2 + jB_2 = (R_D + jX_2)^{-1} , \tag{3.7.6}$$

which yields

$$G_2 = \frac{R_D}{R_D^2 + X_2^2} \tag{3.7.7}$$

$$B_2 = - \frac{X_D}{R_D^2 + X_2^2} . \tag{3.7.8}$$

Setting $G_2 = 1/R_T$ in (3.7.7), we obtain

$$X_2 = (R_D R_T - R_D^2)^{1/2} . \tag{3.7.9}$$

since $X_2 = X_M + X_D$, the required X_M is

$$X_M = (R_D R_T - R_D^2)^{1/2} - X_D . \tag{3.7.10}$$

Since X_D is negative, X_M must be positive; i.e., a matching inductor $L_M = X_M/\omega$ must be used.

Using (3.7.9) in (3.7.8) and setting $B_M = - B_2$, we obtain

$$B_M = \left[\frac{1}{R_T R_D} - \frac{1}{R_T^2} \right]^{1/2} . \tag{3.7.11}$$

Since B_M is positive, a matching capacitor $C_M = B_M/\omega$ is required.

Because R_D is actually a function of $\tilde{I}_0$, we must specify $\tilde{I}_0$ for the matched condition $Z_3 = R_T$. The power supplied by the source to the discharge is

$$\overline{P}_T = \frac{1}{4} \frac{|\tilde{V}_T|^2}{R_T} . \tag{3.7.12}$$

The power absorbed by the discharge is

$$\overline{P}_{rf} = \frac{1}{2} \tilde{I}_0^2 R_i + \frac{1}{2} \tilde{V}_{p0} \tilde{I}_0 . \tag{3.7.13}$$

Equating these powers and solving for $\tilde{I}_0$, we obtain

$$\tilde{I}_0 = \frac{1}{2}\left[\left[\frac{|\tilde{V}_T|^2}{R_T R_i} + \frac{\tilde{V}_{p0}^2}{R_i^2}\right]^{1/2} - \frac{\tilde{V}_{p0}}{R_i}\right]. \tag{3.7.14}$$

Using $R_D = R_i + \tilde{V}_{p0}/\tilde{I}_0$, we obtain

$$R_D = R_i \frac{\left[\frac{|\tilde{V}_T|^2}{R_T R_i} + \frac{\tilde{V}_{p0}^2}{R_i^2}\right]^{1/2} + \frac{\tilde{V}_{p0}}{R_i}}{\left[\frac{|\tilde{V}_T|^2}{R_T R_i} + \frac{\tilde{V}_{p0}^2}{R_i^2}\right]^{1/2} - \frac{\tilde{V}_{p0}}{R_i}}. \tag{3.7.15}$$

In the limit of mainly ion power losses (high discharge voltage), $\tilde{V}_{p0}/\tilde{I}_0 \ll R_i$ and

$$\tilde{I}_0 = \frac{1}{2}\frac{|\tilde{V}_T|}{(R_T R_i)^{1/2}}, \tag{3.7.16}$$

$$R_D = R_i . \tag{3.7.17}$$

In the opposite limit of mainly electron power losses,

$$\tilde{I}_0 = \frac{|\tilde{V}_T|^2}{4R_T \tilde{V}_{p0}} \tag{3.7.17}$$

and

$$R_D = 4R_T \frac{\tilde{V}_{p0}^2}{|\tilde{V}_T|^2}. \tag{3.7.18}$$

The source voltage $\tilde{V}_T$ is out of phase with the discharge current $\tilde{I}$. It can be shown that for the circuit in Fig. 3.13 under matched conditions,

$$\cos\phi_T = \frac{2(\tilde{V}_{p0}+\tilde{I}_0 R_i)}{\tilde{V}_{T0}}, \tag{3.7.19}$$

where ϕ_T is the phase angle between the source voltage and the discharge current.

We note that an L-network cannot be used to match a discharge having $R_D > R_T$. This is seen in Fig. 3.14 where the constant R_D vertical line no longer intersects the constant $G = 1/R_T$ circle; a

real solution (3.7.9) for X_2 no longer exists. To achieve a match in this case the order of B_M and X_M must be inverted, putting B_M nearest the discharge. A three element (T or Π) network can be used to match any discharge. The three elements are not uniquely determined by the condition of achieving a match.

A stray capacitance C_w across terminals a-b in Fig. 3.13 is often present in real discharges. An L-network can still be used to achieve a match in this case.

3.8. Conclusions

The equations for the basic model of the capacitive rf discharge are summarized below:

$$\frac{2u_B}{Nd} = K_{iz}(T_e) \tag{3.8.1}$$

$$n = \frac{\tilde{I}_0}{eA\tilde{u}_0} \tag{3.8.2}$$

$$\bar{P}_{rf} = 2\frac{u_B}{\tilde{u}_0}\tilde{I}_0\mathcal{E}_L + \frac{3\tilde{I}_0^2 u_B}{2\varepsilon_0\omega^2 A} \tag{3.8.3}$$

$$\tilde{V} \approx \frac{2\tilde{u}_0\tilde{I}}{j\omega^2\varepsilon_0 A} \tag{3.8.4}$$

$$\bar{V}_{ps} = \frac{3}{8}\,|\tilde{V}| \tag{3.8.5}$$

$$d = l - \frac{2\tilde{u}_0}{\omega}\,. \tag{3.8.6}$$

In these equations,

$$\tilde{u}_0 = \omega\tilde{s}_0 = \left[\frac{4e\,\mathcal{E}_L\,u_B}{m\nu_m d}\right]^{1/2},$$

$$u_B = \left[\frac{eT_e}{M}\right]^{1/2},$$

$$u_e = \left[\frac{8eT_e}{\pi m}\right]^{1/2},$$

$$\nu_m = NK_m ,$$

and the rate constants $K_{iz}(T_e)$ and $K_m(T_e)$ are given for Maxwellian electrons in argon gas in Figs. 3.6 and 3.10, respectively. Given the control parameters $\tilde{I} = \tilde{I}_0 e^{j\phi_0}$, ω, N and l, the algebraic set (3.8.1)-(3.8.6) can be solved for T_e, n, $\bar{P}_{rf}$, $\tilde{V}$, $\bar{V}_{ps}$, $\tilde{u}_0$, $\tilde{s}_0 = \bar{s}$, and d, provided N exceeds a minimum neutral density $N_{\min}$. Alternately, $\bar{P}_{rf}$ or $\tilde{V}_0$ can be used instead of $\tilde{I}_0$ as the electrical control parameter.

We have shown that the time-varying discharge dynamics appears linear to an external observer; i.e., a sinusoidal current source at frequency ω produces a sinusoidal external voltage at frequency ω, with no harmonic generation. However, the time-varying dynamics of the sheaths within the discharge are nonlinear. This leads to second harmonic voltage generation within the discharge that is unseen by an external observer. We have also shown how to use a matching network to transfer maximum power from the rf source to the discharge.

We now verify several assumptions of the basic model. The dc voltage (3.6.9) across the sheath is typically of order 100 volts. The ratio of Debye length to sheath thickness is

$$\frac{\lambda_D}{\tilde{s}_0} = \left[\frac{3T_e}{4\bar{V}_{ps}}\right]^{1/2} \tag{3.8.7}$$

Since T_e is of order a few volts, the sheath is tens of Debye lengths thick.

In a real sheath, the electron density is not identically zero, but is determined by the Boltzmann factor:

$$n_e(z,t) = n \exp(-\Phi(z,t)/T_e) , \tag{3.8.8}$$

where $\Phi(z,t)$ is the potential in the sheath with respect to the plasma-sheath interface. Integrating (3.3.2) once to obtain

$$\Phi = \frac{en}{2\varepsilon_0}(s_a - z)^2 \tag{3.8.9}$$

and substituting this in (3.8.8) we obtain

$$n_e = n \exp\left[-\frac{(s_a - z)^2}{\lambda_D^2}\right]. \tag{3.8.10}$$

We see that $n_e \ll n$ a few Debye lengths into the sheath from the plasma-sheath interface at s_a. This justifies assumption (4).

The mean electric field $\bar{E}$ within the sheath can be estimated from (3.3.2)

$$\bar{E} \approx \frac{en}{2\varepsilon_0} s_a \ . \tag{3.8.11}$$

The ion transit time t_i across the sheath is determined from the relation

$$s_a \approx \frac{1}{2}\left[\frac{e\bar{E}}{M}\right] t_i^2 \tag{3.8.12}$$

which yields $t_i \approx 2/\omega_i$. For $\omega \gg \omega_i$, we have $\omega t_i \gg 1$, which verifies assumption (2).

The ratio of ion conduction current to displacement current in the sheath is found using (3.3.21) and (3.3.23):

$$\frac{\bar{I}_i}{\tilde{I}_0} = \frac{u_B}{\tilde{u}_0} \ . \tag{3.8.13}$$

Substituting (3.5.5) and (3.8.7) in (3.8.13) and writing u_B and λ_D in terms of n and T_e, we obtain

$$\frac{\bar{I}_i}{\tilde{I}_0} = \frac{\omega_i}{\omega}\left[\frac{3T_e}{4\bar{V}_{ps}}\right]^{1/2} . \tag{3.8.14}$$

Since $\omega \gg \omega_i$ and $\bar{V}_{ps} \gg T_e$, we find that $\bar{I}_i \ll \tilde{I}_0$; i.e., the conduction current in the sheath is small compared to the displacement current, which is the condition for a capacitive discharge.

REFERENCES

Fermi, E. (1949). Phys. Rev. 75, 1169.

Godyak, V. A. (1972). *Sov. Phys.-Tech. Phys.* 16, 1073.

Godyak, V. A. (1976). *Sov. J. Plasma. Phys.* 2, 78.

Godyak, V. A. (1986). *Soviet Radio Frequency Discharge Research, Delphic Associates, Inc., Falls* Church, Virginia.

Godyak, V. A. and A. A. Kuzovnikov (1975). *Sov. J. Plasma Phys.* 1, 276.

Godyak, V. A. and O. A. Popov (1979). *Sov. J. Plasma Phys.* 5, 227.

Taillet, J. (1969). *Am. J. Phys.* 37, 423.

Lichtenberg, A. J. and M. A. Lieberman (1983). *Regular and Stochastic Motion, Springer-Verlag,* New York.